© 2016. Published by The Company of Biologists Ltd | Development (2016) 143, 4016-4026 doi:10.1242/dev.141812

RESEARCH ARTICLE

Tril targets Smad7 for degradation to allow hematopoietic specification in *Xenopus* embryos

Yangsook Song Green[1], Sunjong Kwon[2,‡], Mizuho S. Mimoto[2,*], Yuanyuan Xie[1] and Jan L. Christian[1,§]

ABSTRACT

In *Xenopus laevis*, bone morphogenetic proteins (Bmps) induce expression of the transcription factor Gata2 during gastrulation, and Gata2 is required in both ectodermal and mesodermal cells to enable mesoderm to commit to a hematopoietic fate. Here, we identify *tril* as a Gata2 target gene that is required in both ectoderm and mesoderm for primitive hematopoiesis to occur. Tril is a transmembrane protein that functions as a co-receptor for Toll-like receptors to mediate innate immune responses in the adult brain, but developmental roles for this molecule have not been identified. We show that Tril function is required both upstream and downstream of Bmp receptor-mediated Smad1 phosphorylation for induction of Bmp target genes. Mechanistically, Tril triggers degradation of the Bmp inhibitor Smad7. Tril-dependent downregulation of Smad7 relieves repression of endogenous Bmp signaling during gastrulation and this enables mesodermal progenitors to commit to a blood fate. Thus, Tril is a novel component of a Bmp-Gata2 positive-feedback loop that plays an essential role in hematopoietic specification.

KEY WORDS: Bmp, Gata2, Tril, Smad7, Primitive hematopoiesis

INTRODUCTION

During embryogenesis, successive phases of hematopoiesis generate blood cells (Baron et al., 2012). The first phase of blood development, primitive hematopoiesis, begins when a subset of mesodermal cells commit to a blood fate during gastrulation. These progenitors differentiate primarily as red blood cells (RBCs). Primitive blood is generated in the yolk sac in mammalian embryos and in the ventral blood island (VBI) in amphibians. Subsequent waves of blood development, termed definitive hematopoiesis, generate multipotent hematopoietic stem cells.

Signals from non-hematopoietic cell niches play an essential role in directing primitive hematopoiesis (Drevon and Jaffredo, 2014). In mouse and chick, hematopoietic mesoderm cannot autonomously differentiate as blood when cultured in isolation, but requires non-cell-autonomous signals transmitted from visceral endoderm in order to do so (Belaoussoff et al., 1998; Wilt, 1965). In *Xenopus*, ectodermal cells provide this signal. When ventral mesoderm is explanted at early gastrula stages and cultured in isolation until the tailbud stage, it fails to form blood unless it is co-cultured with ectoderm (Maeno et al., 1994). By the late gastrula stage, transmission of the ectodermal signals required for blood formation is complete and isolated mesodermal cells can differentiate as RBCs (Mimoto et al., 2015).

Bone morphogenetic proteins (Bmps) are expressed in ectoderm and ventral mesoderm during gastrulation, and are required for cells to adopt ventral fates (Dale et al., 1992; Lyons et al., 1992), including blood (Graff et al., 1994; Maeno et al., 1994). Bmps also function at later stages to prevent bipotential progenitors from choosing the endothelial rather than the erythroid lineage (Myers and Krieg, 2013). Bmps are believed to comprise part of the non-cell-autonomous signal that is transmitted from the ectoderm to the mesoderm to enable it to form blood (Kumano et al., 1999; Maeno, 2003; Tran et al., 2010). Consistent with this idea, mesodermal progenitors of the anterior (a)VBI reside in a dorsal region of the embryo that is devoid of Bmp signaling at the onset of gastrulation, but then migrate beneath the ectoderm, which is rich in Bmps, before committing to an erythroid fate (Ciau-Uitz et al., 2010).

Gata2 is a Bmp target gene that encodes a transcription factor required in both ectoderm and mesoderm to induce expression of genes required for hematopoietic commitment (Dalgin et al., 2007; Liu et al., 2008; Mimoto et al., 2015; Walmsley et al., 1994). In the present study, we identified the Gata2 target gene *tril* (*tlr4 interactor with leucine-rich repeats*) as being required in both ectoderm and ventral mesoderm for primitive hematopoiesis. Tril functions cell-autonomously to downregulate protein levels of the Bmp inhibitor, Smad7, in both germ layers during gastrulation, thereby relieving repression of endogenous Bmp signaling to enable the mesoderm to be specified as blood.

RESULTS

tril is a downstream target of Gata2 that is expressed in mesoderm and ventral ectoderm during gastrulation

We performed a microarray to identify Gata2 target genes in ectoderm explanted from *Xenopus* gastrulae (Fig. 1A) (Mimoto et al., 2015). Expression of Gata2 was upregulated or knocked down in two-cell embryos. Ectodermal explants were dissected at the onset of gastrulation (stage 10), and cultured until the late gastrula stage (st. 12) when RNA was isolated for microarray analysis. We identified *tril* as a gene whose expression was reduced in the absence of Gata2 and enhanced when Gata2 was overexpressed (Fig. 1A). Tril is a transmembrane protein that functions as a co-receptor for Toll-like receptor (Tlr)3 and Tlr4 to mediate innate immune responses in the brain of adult mammals (Carpenter et al., 2009, 2011; Wochal et al., 2014). The extracellular domain contains multiple leucine-rich repeats (LRRs) and a fibronectin type III domain (FN), while the intracellular domain (ICD) contains no known signaling motifs (Fig. 1A). We used quantitative PCR (qPCR) to verify that *tril* expression was reduced in ectodermal explants isolated from Gata2 morphants and showed that *tril*

[1]Department of Neurobiology and Anatomy and Internal Medicine, Division of Hematology and Hematologic Malignancies, University of Utah, School of Medicine, Salt Lake City, UT 84132, USA. [2]Department of Cell and Developmental Biology, Oregon Health and Sciences University, School of Medicine, Portland, OR 97239-3098, USA.
‡Present address: Department of Biomedical Engineering, CL3G Oregon Health & Science University, Portland, OR 97201, USA. *Present address: Department of Internal Medicine, University of Chicago Hospitals, Chicago, IL 60637, USA.

§Author for correspondence (jan.christian@neuro.utah.edu)

J.L.C., 0000-0003-3812-3658

Received 5 July 2016; Accepted 1 September 2016

Development (2016) 143, 4016-4026 doi:10.1242/dev.141812

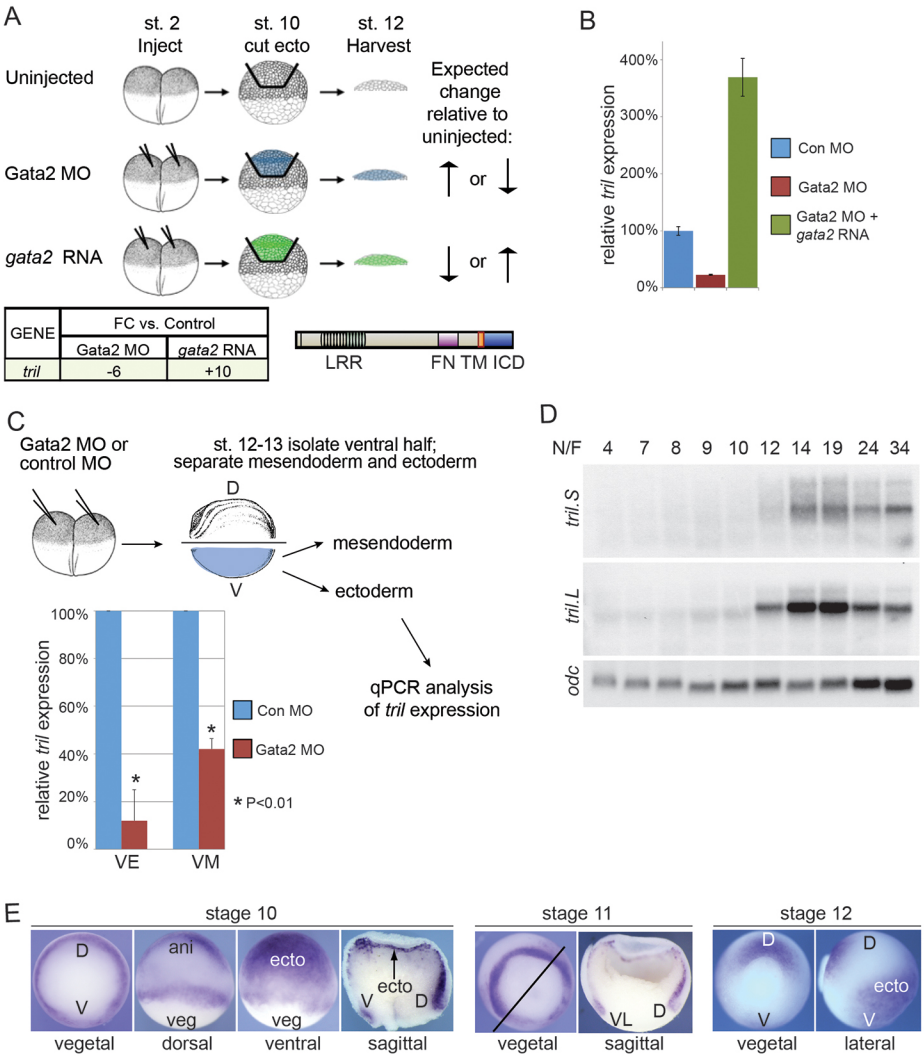

Fig. 1. *tril* is a Gata2 target gene. (A) Illustration of microarray strategy, Tril protein domains and table showing fold change (FC) in expression of *tril* relative to uninjected embryos. Tril contains an extracellular domain with leucine-rich repeats (LRR) and a fibronectin type III domain (FN), a transmembrane (TM) domain and an intracellular domain (ICD). (B) qPCR analysis of *tril* expression in 10 pooled ectodermal explants isolated at stage 10 from embryos injected with control (Con) MO (40 ng), Gata2 MO (40 ng) or Gata2 MO and *gata2* RNA (1 ng) together, and then cultured to stage 12. Values are mean±s.d. Results were reproduced in two independent experiments. (C) Gata2 or control MO (40 ng per embryo) was injected into two-cell embryos. At stage 12-13, ventral (V), ectodermal (VE) or mesendodermal (VM) pieces were isolated, RNA was extracted from 10 pooled explants and *tril* expression analyzed by qPCR. Gene expression (mean±s.d., data analyzed by two-tailed *t*-test) quantified from three independent experiments is shown. (D) Northern analysis showing levels of transcripts of the S and L alloalleles of *tril* at different Nieuwkoop and Faber (N/F) stages of development. (E) Expression of *tril* analyzed by WMISH of probes to whole or bisected embryos. Embryo orientation is indicated below each panel. The black bar in the stage 11 embryo on the left illustrates where the bisection occurred in the embryo shown on the right. D, dorsal; V, ventral; ani, animal pole; veg, vegetal pole; ecto, ectoderm; VL, ventrolateral.

expression could be rescued in morphants by co-injection of *gata2* RNA (Fig. 1B).

gata2 is expressed in both mesoderm and ectoderm during gastrulation (Walmsley et al., 1994) and thus we asked whether *tril* is a target of Gata2 in both germ layers. We injected Gata2 MOs into 2-cell embryos, isolated the ventral half of the embryo at the late gastrula stage (st. 12-13), separated the ventral fragment into ectodermal and mesendodermal pieces as illustrated in Fig. 1C, and analyzed expression of *tril* in each tissue by qPCR. *Tril* levels were reduced in ventral ectoderm and mesendoderm of Gata2 morphants compared with controls demonstrating that Gata2 is required for *tril* expression in both germ layers (Fig. 1C).

Two alleles of Xenopus *tril* were identified that share 89% identity at the amino acid level. Northern blot analysis shows that expression of *tril.S* and *tril.L* peaks at the late gastrula stage and persists throughout development (Fig. 1D). Analysis of the spatial pattern of expression of *tril* by whole mount *in situ* hybridization (WMISH) showed that *tril* is expressed in ventral ectoderm and dorsal mesoderm, and more weakly in ventral mesoderm at stages 10 and 11 (Fig. 1E). At stage 12, *tril* is expressed in dorsal mesoderm and ventral ectoderm (Fig. 1E). By contrast, *gata2* is maternally expressed and zygotic transcripts are enriched in ectoderm and ventral mesoderm during gastrulation (Green et al., 2016; Walmsley et al., 1994).

Tril is required for hematopoietic commitment

We generated two MOs that target the 5′ untranslated region (UTR) of both *tril* alleles and used immunoblot analysis to verify that these block the translation of *tril* mRNAs (Fig. S1). To ask whether Tril function is required for blood development, we injected Tril MO1 or MO2 into two ventral blastomeres of 4-cell embryos and examined expression of the RBC marker *hba3.L* (*α-globin*) at stage 34 using WMISH. These ventral cells give rise to the posterior VBI (pVBI), which constitutes the majority of the VBI (Fig. 2A). While most embryos injected with the control MO showed strong expression of *hba3.L* throughout the VBI, embryos injected with Tril MOs showed a dose-dependent reduction in expression of *hba3.L* in the pVBI (Fig. 2A). Expression of *globin* was retained in the aVBI, as expected, since this region is derived from dorsal cells that did not receive the Tril MO. Tril morphants also showed reduced expression of two other RBC markers, *stem cell leukemia* (*scl*) and *gata1* (Fig. 2B).

We then asked whether the reduced *hba3.L* in Tril morphants could be rescued by co-injection of *tril* RNA lacking the 5′UTR. Northern analysis confirmed that expression of *hba3.L* was reduced in Tril morphants (Fig. 2C). Injection of *tril* RNA (100 pg) alone did not cause changes in expression of *hba3.L*, but was sufficient to substantially rescue expression of *hba3.L* when injected together with Tril MO1 (Fig. 2C). Notably, when *tril* RNA was injected into ventral cells at doses higher than 100 pg, a dose-dependent reduction

Development (2016) 143, 4016-4026 doi:10.1242/dev.141812

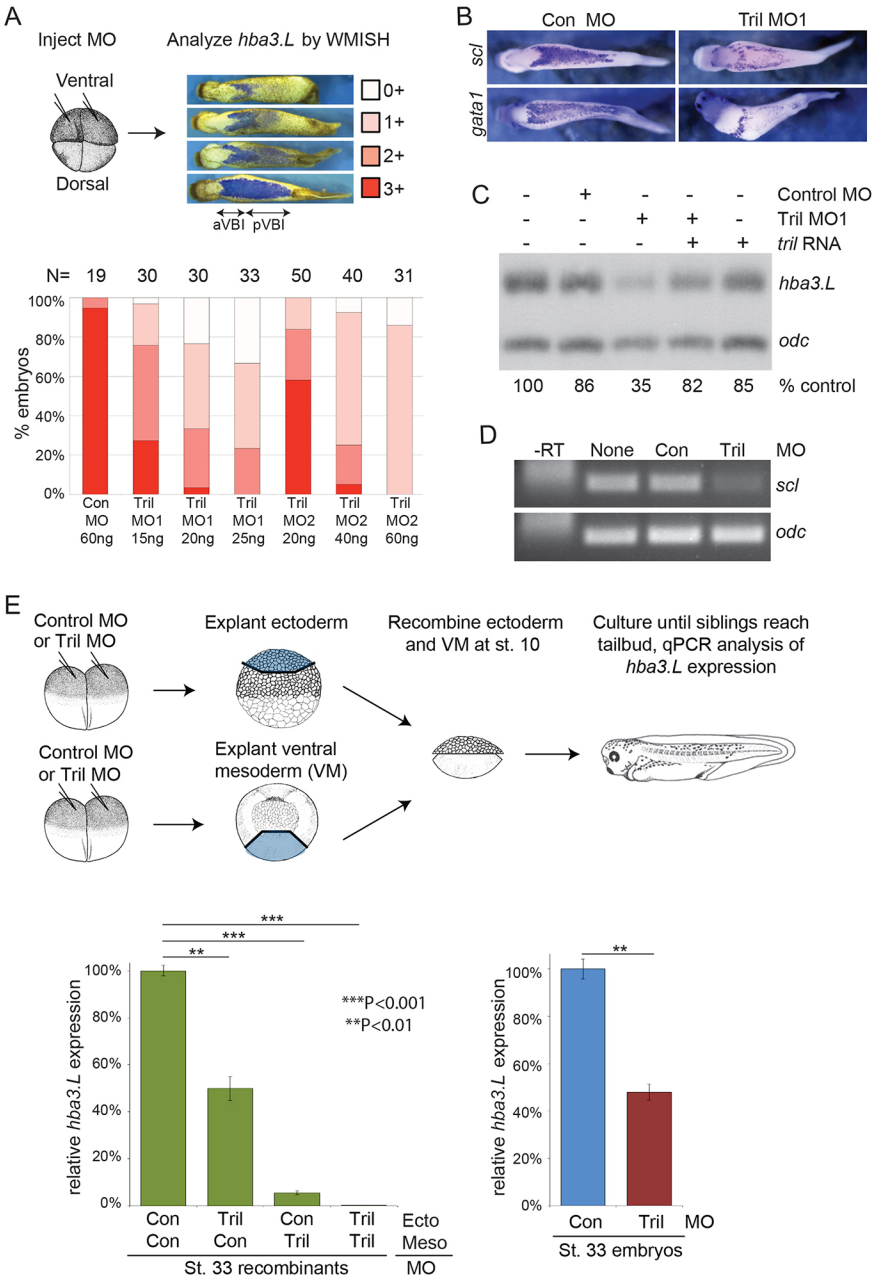

Fig. 2. Tril is required in ectodermal and mesodermal cells for blood commitment. (A,B) Control or Tril MOs (40 ng) were injected into both ventral cells of 4-cell embryos and expression of *hba3.L*, *scl* or *gata1* was analyzed by WMISH at stage 34 in three experiments. *hba3.L* staining in the posterior VBI (pVBI) was scored as absent (0+), weak (1+), very weak (2+) or strong (3+), as illustrated. aVBI, anterior VBI. (C) Control or Tril MO1 (40 ng) and/or *tril* RNA lacking the 5′UTR (100 pg) was injected into two ventral vegetal blastomeres of eight-cell embryos and expression of *hba3.L* was analyzed by northern blotting at stage 34. Levels of *hba3.L* transcripts normalized to *odc* and reported as a percentage of *hba3.L* levels in control embryos are shown below each lane. Results were replicated in three experiments. (D) Control or Tril MO1 (40 ng) was injected into both cells of two-cell embryos and expression of *scl* was analyzed by RT-PCR at stage 15. Results were reproduced in three experiments. -RT, no reverse transcriptase in cDNA synthesis reaction. (E) Control or Tril MO1 (40 ng) was injected into two-cell embryos. At stage 10, ectoderm (ecto) or ventral mesoderm (VM) was explanted and recombined in the combinations indicated below the graph on the right. Expression of *hba3.L* was analyzed in 10 pooled recombinants in each group (left) or in 10 whole sibling embryos (right) at stage 34 by qPCR (mean±s.d., data analyzed by two-tailed *t*-test). Results were reproduced in two independent experiments.

in *hba3.L* transcripts was observed (Fig. S2), demonstrating that precise regulation of Tril levels is crucial for blood development.

To ask whether the defects in blood differentiation in Tril morphants are caused by an earlier failure to commit to a hematopoietic fate, we analyzed expression of *scl*, which serves as a marker of hematopoietic commitment at early neurula stages (Mead et al., 1998). Expression of *scl* was reduced in Tril morphants at stage 15 (Fig. 2D).

Tril function is required in both mesoderm and ectoderm for blood development

A tissue recombination assay was used to test whether Tril is required in ectoderm and/or mesoderm for blood development. Ectoderm was isolated from Tril or control morphants at the beginning of gastrulation (st. 10), recombined with ventral mesoderm from Tril or control morphants and recombinants were co-cultured until sibling embryos reached the tailbud stage (st. 33), when expression of *hba3.L* was analyzed by qPCR (Fig. 2E). *hba3.L* was robustly expressed in recombinants of ventral mesoderm and ectoderm isolated from control morphants but the *hba3.L* level was halved in control mesoderm co-cultured with ectoderm isolated from Tril morphants (Fig. 2E). Furthermore, when ventral mesoderm isolated from Tril morphants was co-cultured with ectoderm from control morphants, expression of *hba3.L* was reduced to ∼5% of the untreated control level (Fig. 2E). A further reduction in *hba3.L* expression was observed when both tissues were derived from Tril morphants (Fig. 2E). Thus, Tril function is required in both ventral mesoderm and, perhaps to a lesser extent, in ectoderm for blood development.

Tril is required upstream and downstream of Smad1 phosphorylation for Bmp target gene expression

Bmp signals must be transduced in both ectoderm and ventral mesoderm during gastrulation in order for primitive hematopoiesis to occur (Kumano et al., 1999; Walters et al., 2001), raising the possibility

Development (2016) 143, 4016-4026 doi:10.1242/dev.141812

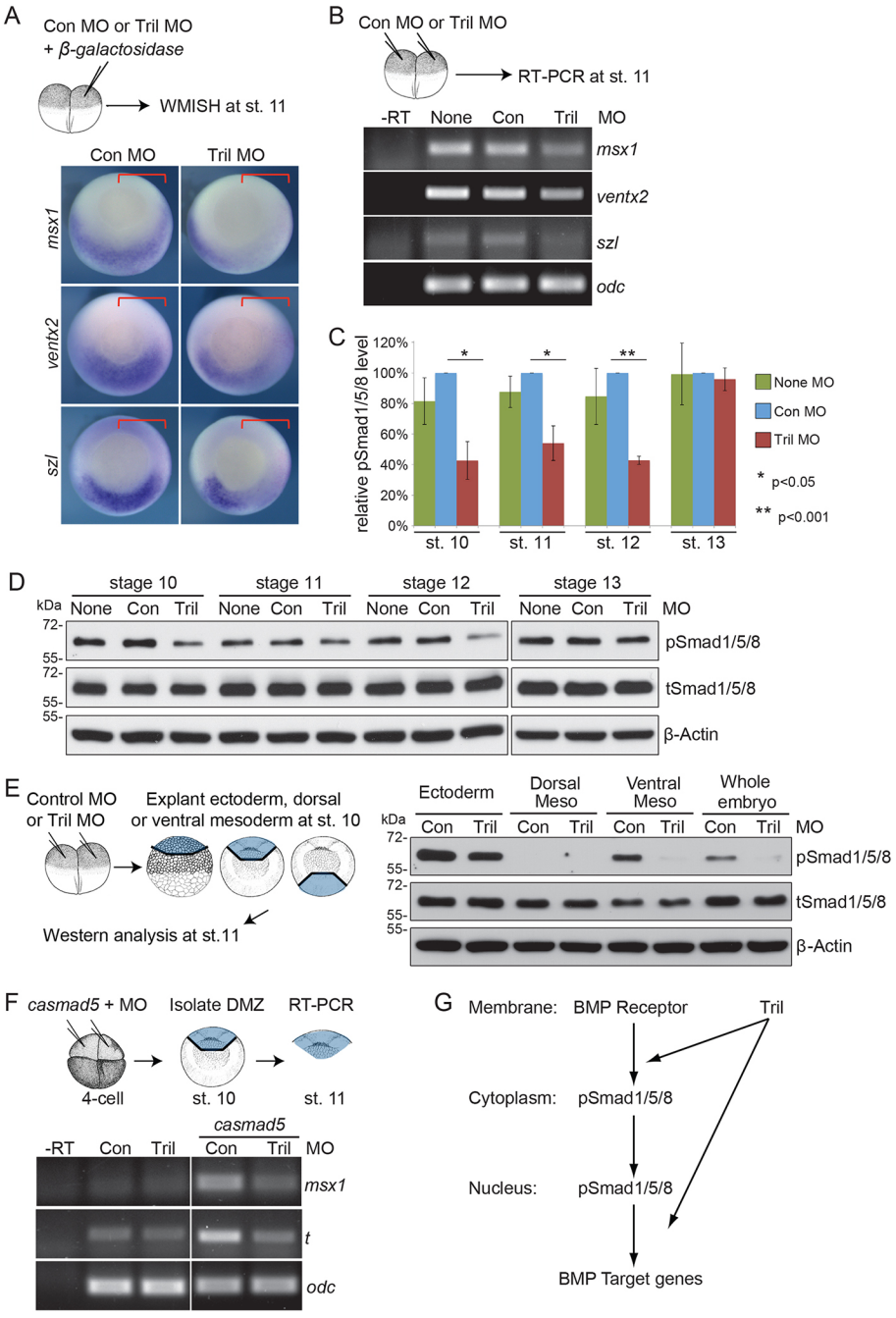

Fig. 3. Tril is required upstream and downstream of Smad1 phosphorylation for Bmp target gene expression. (A) β-galactosidase (*lacZ*) RNA was co-injected with control or Tril MOs (40 ng) as illustrated. Embryos were stained for β-galactosidase activity at stage 11 to identify the half of the embryo that received the MOs (indicated by a red bracket) and expression of Bmp target genes was analyzed by WMISH. (B-E) Tril, control (Con) or no (None) MOs were injected into two-cell embryos. (B) Expression of *msx1*, *ventx2*, *szl* and *odc* analyzed by RT-PCR. Results were reproduced in three experiments. -RT, no reverse transcriptase in cDNA synthesis reaction. (C,D) Levels of pSmad1/5/8, total Smad1/5/8 (tSmad1/5/8) and β-Actin were analyzed by immunoblot at the indicated stages. A representative blot (D) and normalized data (levels of Smad1/5/8 normalized to β-Actin) from three independent experiments (values are mean±s.d.) (C) are shown. (E) The indicated tissues were explanted from 10 embryos in each group and levels of pSmad1/5/8, tSmad1/5/8 and β-Actin analyzed by immunoblot. Results were reproduced in two experiments. (F) Tril or control MOs were injected alone, or together with RNA encoding caSmad5, into both dorsal cells of four-cell embryos. The dorsal quadrant of the embryo was explanted at stage 10 and cultured until stage 11, at which time expression of *t*, *msx1* and *odc* was analyzed by RT-PCR. Results were reproduced in three independent experiments. (G) Tril functions both upstream and downstream of pSmad1/5/8 to enhance Bmp signaling.

that Tril functions to promote Bmp signaling. To test this, we co-injected Tril or control MOs, together with RNA encoding β-galactosidase (as a lineage tracer), into one cell of two-cell embryos. Embryos were cultured until stage 11 when they were stained for β-galactosidase activity followed by analysis of Bmp target gene expression by WMISH. Expression of *msx1*, *ventx2* and *szl* was reduced in cells on the side of the embryo that received Tril MOs compared with the control side and also compared with embryos injected with control MOs (Fig. 3A, injected side marked by a red bar). We also injected Tril MOs into both cells of two-cell embryos and analyzed expression of Bmp target genes by semi-quantitative RT-PCR at stage 11. Expression of *msx1*, *ventx2* and *szl* was reduced in Tril morphants (Fig. 3B).

To further test whether Tril is required for Bmp signal transduction, we analyzed levels of phosphorylated (p)Smad1/5/8, which provides a direct read out of Bmp pathway activation. Tril MOs were injected into both cells of two-cell embryos and levels of pSmad1/5/8, total Smad1/5/8 and β-Actin were analyzed by immunoblotting at stages 10-13. Relative levels of pSmad1/5/8 normalized to β-Actin were strongly reduced in Tril morphants during early- and mid-gastrulation (st. 10-12) but returned to control levels by the end of gastrulation (st. 13) (Fig. 3C,D). By contrast, levels of phosphorylated Erk were unchanged in Tril morphants (Fig. S3), showing that cell signaling is not globally impaired.

To determine whether Tril is required for Bmp signaling in ectoderm and/or mesoderm, pSmad1/5/8 levels were analyzed in pooled ectodermal, dorsal or ventral mesendodermal fragments dissected from Tril or control morphants at stage 11. pSmad1/5/8 was not detected in dorsal explants, because these cells have minimal endogenous Bmp activity. Levels of pSmad1/5/8 were

Development (2016) 143, 4016-4026 doi:10.1242/dev.141812

reduced in ectodermal and ventral mesendodermal cells of Tril morphants relative to controls (Fig. 3E).

We have previously shown that levels of *bmp2*, *bmp4* and *bmp7* transcripts are not reduced in Gata2 morphants (Dalgin et al., 2007; Mimoto et al., 2015), but the current data showing that Bmp pathway activation is reduced when expression of the Gata2 target gene *tril* is knocked down, led us to re-examine whether Bmp signal transduction is reduced in Gata2 morphants. We found that levels of pSmad1/5/8 were reduced in ventral ectoderm and mesoderm of Gata2 morphants during early- and mid-gastrula stages (Fig. S4). Collectively, these results show that Tril is required downstream of Gata2 for full activation of the Bmp pathway.

If Tril is only required for Bmp receptor-mediated phosphorylation of Smad1/5/8, then it should be possible to rescue expression of Bmp target genes in Tril morphants by expressing a constitutively active (ca) form of Smad1, Smad5 or Smad8. To test this possibility, RNA encoding caSmad5, in which the C-terminal SSXS motif has been changed to an SDVD motif (Tsukamoto et al., 2014), was injected near the dorsal marginal zone (DMZ) of four-cell Tril morphants or control embryos. The DMZ was explanted from early gastrulae (st. 10) and cultured to the mid-gastrula stage (st. 11), at which time expression of Bmp target genes was analyzed (illustrated in Fig. 3F). We expressed caSmad5 in the dorsal region because it has little endogenous Bmp signaling (Fig. 3E). Ectopic expression of caSmad5 led to upregulation of *msx1* and *t* (*xbra*) in dorsal cells of control morphants, but not Tril morphants (Fig. 3F). Thus, Tril is required both upstream and downstream of Bmp receptor-mediated Smad1/5/8 phosphorylation for induction of Bmp target genes (Fig. 3G).

Tril inhibits accumulation of Smad7 protein

The inhibitory Smads, Smad6 and Smad7, constrain Bmp signaling upstream of receptor-mediated phosphorylation of Smad1/5/8 (Murakami et al., 2003; Souchelnytskyi et al., 1998) but also block transcriptional responses downstream of pSmad1/5/8 in the nucleus (Bai and Cao, 2002; Lin et al., 2003). Our results showing that Tril acts both upstream and downstream of pSmad1/5/8 raised the possibility that it does so by negatively regulating Smad6 and/or Smad7. To test this possibility, we first asked whether loss of endogenous Tril leads to changes in the subcellular localization of Smad6 and Smad7. We were unable to detect endogenous Smad6 or Smad7 using available antibodies and thus analyzed ectopically expressed epitope-tagged Smads for immunostaining and western analysis. We injected Tril or control MOs into two-cell embryos and then injected *myc*-tagged *smad6* or *smad7* RNA (50 pg), together with membrane-tagged RFP (memRFP) RNA into a single blastomere at the four-cell stage. Ectoderm was explanted and immunostained at stage 11 (illustrated in Fig. 4A). Smad6 was detected in the nucleus, at the plasma membrane and diffusely throughout the cytoplasm, with no apparent difference in intensity of staining or subcellular localization in controls relative to Tril morphants (Fig. 4A). Smad7 staining was readily detected in explants isolated from Tril morphants but was barely visible in explants from control morphants when imaged under identical conditions (Fig. S5). When the signal was enhanced in control morphants, Smad7 was detected primarily in the cytoplasm and at the plasma membrane (Fig. 4A) or was evenly distributed throughout the cytoplasm, nucleus and membrane in most explants (Fig. 4B), but was present primarily in the nucleus in most explants isolated from Tril morphants (Fig. 4A,B). Next, we compared levels of Smad7-Myc and Smad6-Myc protein on immunoblots. Steady-state levels of Smad7 protein were 3- to 6-fold higher in Tril morphants than in controls in three independent experiments, whereas no difference was observed in the level of Smad6 protein in Tril morphants relative to controls (Fig. 4C). Smad7 protein levels were upregulated in embryos injected with either of the two MOs specific for Tril (Fig. S6). Upregulation of Smad7 protein is not due to enhanced transcription or RNA stability since levels of *smad7* RNA were slightly lower in Tril morphants relative to controls (Fig. 4D), which is expected given that *smad7* is a Bmp target gene (Nakayama et al., 1998) and Bmp signaling is reduced in Tril morphants. Thus, Tril selectively and post-transcriptionally inhibits accumulation of Smad7, but not Smad6, protein, particularly within the nuclear compartment.

To determine whether excessive accumulation of Smad7 is responsible for reduced Bmp activity in Tril morphants, we first tested whether overexpression of Smad7 could synergize with knockdown of Tril to inhibit endogenous Bmp signaling. Embryos were injected with a low dose of RNA (25 pg) encoding Smad7 that had no effect on pSmad1/5/8 levels in control embryos (Fig. 4E). In Tril morphants, levels of pSmad1/5/8 were reduced to 64% of control levels in the absence of ectopic Smad7 and were further reduced to 25% of control levels in the presence of ectopic Smad7 (Fig. 4E).

Next, we tested whether knocking down expression of Smad7 was sufficient to rescue Bmp target gene expression and blood formation in Tril morphants. A previously characterized Smad7 MO (Choi et al., 2008) was co-injected together with control or Tril MOs into both ventral cells of four-cell embryos. Expression of the Bmp target gene *szl* and the blood differentiation marker *hba3.L* was analyzed by qPCR when embryos reached stage 11 and stage 33, respectively. Levels of *szl* and *hba3.L* transcripts were reduced by 25% and 50%, respectively, in Tril morphants relative to controls, and were partially but significantly rescued by co-injection of the Smad7 MO (Fig. 4F). Notably, Smad7 is maternally expressed and the Smad7 MO can not deplete maternal stores of Smad7 protein. This may explain our inability to fully rescue gene expression in Tril morphants. Our data support the conclusion that Tril functions to reduce endogenous Smad7 protein levels during gastrulation, and that relief of Smad7-mediated repression of Bmp signaling enables mesoderm to commit to a blood fate (Fig. 4G).

Tril promotes degradation of Smad7 protein

To determine whether accumulation of Smad7 in Tril morphants is caused by impaired degradation, we compared the turnover rate of Smad7-Myc in control and Tril morphants in the presence and absence of cycloheximide (CHX). Embryos were injected with *smad7-myc* RNA together with control or Tril MOs at the two-cell stage. Beginning at stage 11, they were cultured in the presence or absence of CHX for 1, 2 or 3 h before harvesting for immunoblot analysis of Smad7-Myc levels. In control embryos, when protein synthesis was intact, Smad7 protein decayed over time, reaching barely detectable levels within 3 h. However, when new protein synthesis was blocked, Smad7-Myc protein decayed more slowly and was still detectable after 3 h of incubation (Fig. 5A). Thus, Smad7 protein is rapidly turned over during mid- to late-gastrula stages and the protein(s) that trigger its degradation must be actively translated during that period. In Tril morphants, Smad7 protein decayed more slowly than in controls when protein synthesis was intact (Fig. 5A), suggesting that Tril promotes Smad7 degradation. Furthermore, unlike in control embryos, in Tril morphants, Smad7 decayed at approximately the same rate in the presence and absence of new protein synthesis (Fig. 5A). The observation that protein synthesis-dependent degradation of Smad7 is rescued by removal of Tril suggests that Tril (or another protein that functions downstream of Tril) is responsible for degradation of Smad7 during the mid- to

Development (2016) 143, 4016-4026 doi:10.1242/dev.141812

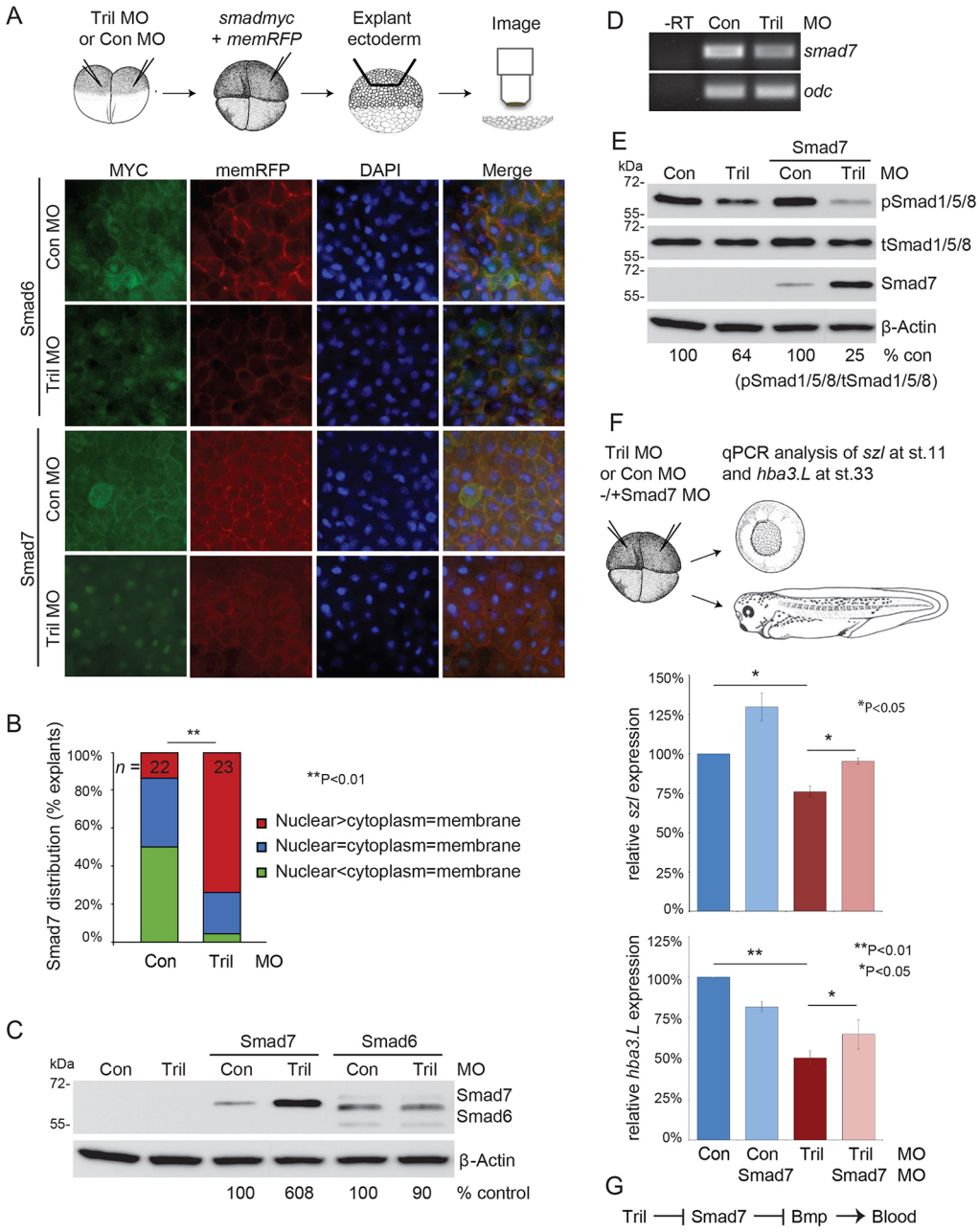

Fig. 4. Tril enhances Bmp signaling by inhibiting accumulation of Smad7 but not Smad6 protein. (A,B) Tril or control MOs (40 ng), and RNAs encoding Smad7-Myc or Smad6-Myc, together with RNA encoding membrane-targeted RFP (memRFP) were injected as illustrated. Ectoderm was explanted from 5-10 embryos in each group at stage 11 and immunostained for Myc and RFP. Representative immunostaining is shown in A (all images taken under identical conditions except that a longer exposure of Smad7-Myc is shown for control embryos relative to Tril morphants) and results are quantified in B. Differences in subcellular localization of Smad7 were compared using a two-way ANOVA followed by a Bonferroni multiple comparisons test. Results were reproduced in three independent experiments. (C) RNA (25 pg) encoding Smad6-Myc or Smad7-Myc was injected into two-cell embryos along with control or Tril MOs. Immunoblots of lysates from stage 11 embryos (10 per group) were probed with anti-Myc antibodies, and then reprobed for β-Actin. Levels of Smad7 or Smad6 in Tril morphants, normalized to β-Actin are reported as a percentage of levels in control morphants below each lane. Results were replicated in three experiments. (D) MOs were injected into two-cell embryos and ectoderm was dissected from 10 embryos in each group at stage 10. Expression of endogenous *smad7* and *odc* was analyzed by semi-quantitative RT-PCR at stage 11. Results were reproduced in three independent experiments. (E) MOs were injected into two-cell embryos either alone or with 25 pg Smad7-Myc RNA. Immunoblots of stage 11 lysates were probed with antibodies specific for pSmad1/5/8, tSmad1/5/8, Myc and β-Actin. Levels of pSmad1/5/8 in Tril morphants, normalized to tSmad1/5/8, are reported as a percentage of pSmad1/5/8 levels in control morphants below each lane. Results were replicated in three experiments. (F) Tril or control MOs (20 ng) were injected alone or together with Smad7 MO (20~25 ng) into both ventral cells of embryos at the four-cell stage and gene expression was analyzed by qPCR as illustrated. Levels of *szl* or *hba3.L* transcripts are reported as a percentage of control levels. Values are mean±s.d. (G) Tril inhibits Smad7 to relieve repression of Bmp activity during blood development.

late-gastrula stage. This time period coincides with the developmental window during which *tril* transcript levels are rapidly increasing (Fig. 1D).

Smad7 protein stability is tightly regulated through interactions with a variety of binding partners and via post-translational modifications, such as ubiquitylation (Yan and Chen, 2011). One

Development (2016) 143, 4016-4026 doi:10.1242/dev.141812

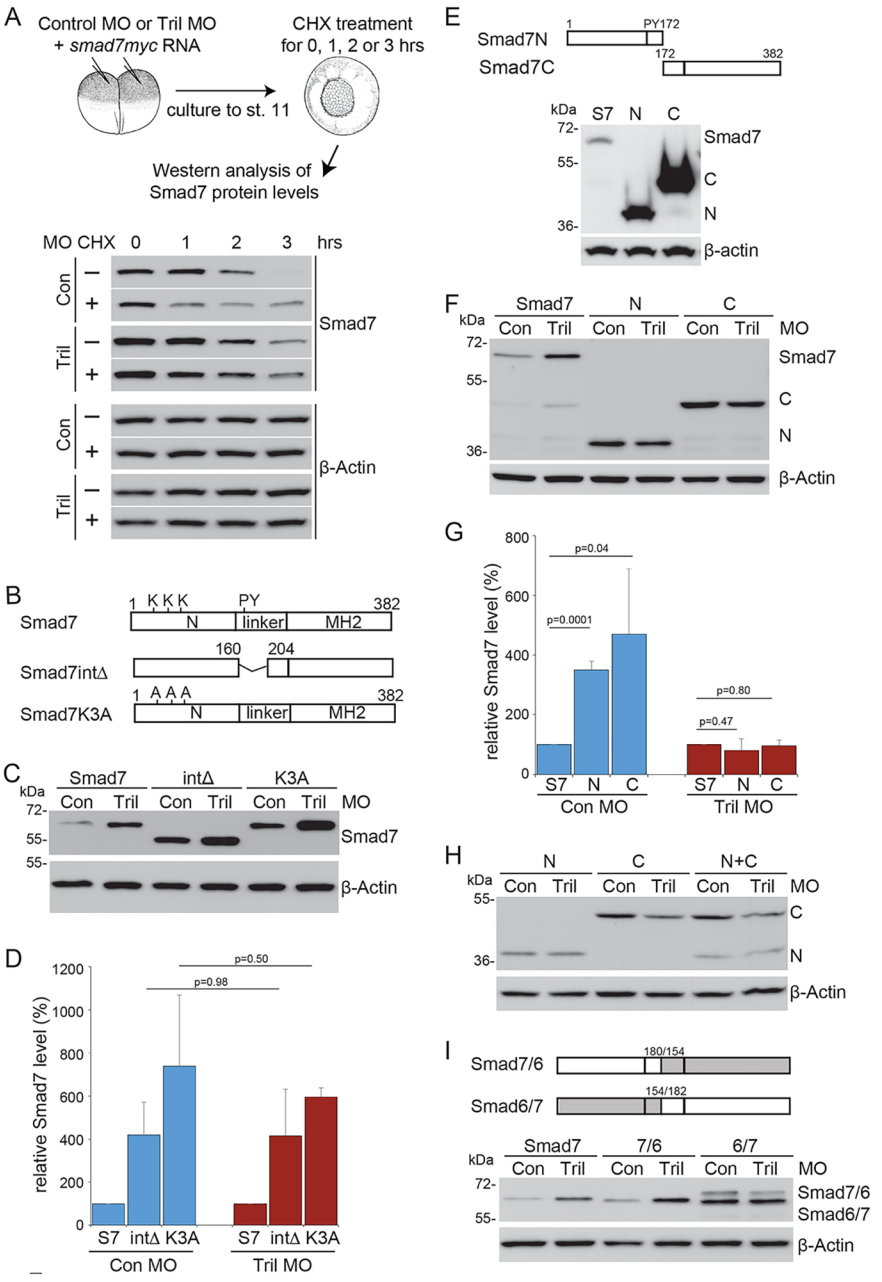

Fig. 5. Tril triggers degradation of Smad7 protein through a mechanism that requires both the N- and C-terminal regions of Smad7. (A) RNA encoding Smad7-Myc (25 pg) was injected along with control or Tril MOs and embryos were incubated in medium containing 30 µg/ml cycloheximide (CHX) or vehicle beginning at stage 11. Immunoblots of lysates collected at 0, 1, 2 and 3 h after CHX treatment were probed with antibodies specific for Myc, and then reprobed for β-Actin. Results were reproduced in three experiments. Gels were run with a single zero time point sample in the middle of the gel and 1-3 h samples (±CHX) on either side. Thus, the zero time point band for each morphant is duplicated but reversed horizontally in the ±CHX lanes. (B) Smad7 protein domain structure. (C,D) RNA encoding Smad7-Myc (25 pg), Smad7intΔMyc (22 pg) or Smad7K3AMyc (25 pg) was injected into two-cell embryos along with control or Tril MOs. Immunoblots of lysates from 10 pooled stage 11 embryos in each group were probed with anti-Myc antibodies, and then reprobed for β-Actin. A representative blot (C) and normalized data (levels of mutant Smad7, normalized to β-Actin and reported as a percentage of wild-type Smad7 levels) from three independent experiments (values are mean±s.d.) (D) are shown. (E) Equivalent molar amounts of *smad7*, *smad7*-N or *smad7*-C RNA were injected into two-cell embryos. Immunoblots of lysates from stage 11 embryos were probed with anti-Myc antibodies, and then reprobed for β-Actin. (F-H) RNA encoding Smad7-Myc (25 pg), or encoding Smad7-N-Myc (1.4 pg) or Smad7-C-Myc (0.5 pg) alone or both RNAs together was injected into two-cell embryos along with control or Tril MOs. Immunoblots of lysates from stage 11 embryos were probed with anti-Myc antibodies and then reprobed for β-Actin. Representative blots (F,H) and normalized data (levels of mutant Smad7, normalized to β-Actin and reported as a percentage of wild-type Smad7 levels) from three independent experiments (G) (values are mean±s.d.) are shown. (I) RNA encoding Smad7-Myc, Smad7-N/6-C-Myc or Smad6-N/7-C-Myc (25 pg each) was injected into two-cell embryos along with control or Tril MOs. Immunoblots of lysates from stage 11 embryos were probed with anti-Myc antibodies and then reprobed for β-Actin.

pathway for Smad7 degradation involves the ubiquitin ligases Smurf1/2, which bind to a PY motif in the middle linker domain of Smad7 and are recruited to activated Bmp receptors where they ubiquitylate both the receptors and Smad7, targeting them for proteasomal degradation (Ebisawa et al., 2001; Kavsak et al., 2000). To ask whether Smurfs promote degradation of Smad7 and whether this requires Tril, we compared steady-state levels of wild-type Smad7-Myc protein with that of Smad7-Myc variants that are predicted to be unable to interact with, or to be ubiquitylated by, Smurfs. Equivalent molar amounts of RNA encoding Smad7, Smad7intΔ, which lacks the PY binding motif, or Smad7K3A, in which three lysine residues that are predicted to be ubiquitylated by Smurfs (Gronroos et al., 2002) are substituted with alanine residues (Fig. 5B), were injected into two-cell embryos and levels of each protein were analyzed by immunoblot at stage 11. Steady-state levels of Smad7intΔ or Smad7K3A were approximately 4- or 7-fold higher than those of wild-type Smad7 in control embryos, demonstrating that Smurfs promote Smad7 degradation during development (Fig. 5C,D). If Tril is required to stimulate Smurf-dependent degradation of Smad7, then the enhanced accumulation of these mutant forms of Smad7 should be lost in Tril morphants. Contrary to this prediction, although steady-state levels of Smad7intΔ or Smad7K3A were enhanced in Tril morphants relative to controls (Fig. 5C and Fig. S7), there was no difference in the increase of Smad7intΔ or Smad7K3A in Tril morphants when compared with that in controls (Fig. 5D and Fig. S7). Thus, Tril promotes degradation of Smad7 independent of Smurfs.

We next used deletion analysis to identify domains of Smad7 that are required for Tril-dependent degradation. When similar molar amounts of RNA encoding wild-type Smad7, Smad7-N, which contains only the N-terminal domain, or Smad7-C, which lacks the N-terminus, were injected into wild-type embryos, steady-state levels of Smad7-N and Smad7-C were 20- to 60-fold higher than those of wild-type Smad7 (Fig. 5E). We then titrated the amount of

Development (2016) 143, 4016-4026 doi:10.1242/dev.141812

smad7-N or *smad7*-C RNA to find a dose that generated detectable protein on immunoblots but did not saturate the signal. In subsequent experiments, we injected 60-times less *smad7c* RNA (0.5 pg) and 20-times less *smad7*-N RNA (1.4 pg) relative to that encoding Smad7 (25 pg). Unlike wild-type Smad7, which is present at higher levels in Tril morphants than in controls, steady-state levels of Smad7-N and Smad7-C showed no significant change in Tril morphants relative to controls when quantitated from three independent replicates (Fig. 5F and Fig. S8), suggesting that both the N- and C-termini of Smad7 are essential for enhanced stability in Tril morphants. Consistent with this conclusion, steady-state levels of Smad7-N or Smad7-C were significantly higher than wild-type Smad7 levels in control embryos, but were unchanged relative to wild-type Smad7 levels in Tril morphants (Fig. 5G). These data demonstrate that Tril is part of the cellular machinery that prevents excessive accumulation of Smad7 protein via a post-translational mechanism that requires both the N- and C-terminal domains of Smad7.

To ask whether the N- and C-terminal domains of Smad7 can act in trans to prevent accumulation of Smad7, we compared levels of Smad7-N or Smad7-C in embryos co-expressing the two proteins with that in embryos expressing each protein individually. Steady-state levels of Smad7-N and Smad7-C were unchanged in embryos co-expressing both proteins relative to that in embryos expressing each protein individually (Fig. 5H). Because Tril selectively accelerates turnover of Smad7 and not Smad6, we next compared steady-state levels of chimeric proteins consisting of the N-terminus of Smad6 fused to the C-terminus of Smad7 (Smad6/7) or vice versa (Smad7/6; illustrated in Fig. 5I). Steady-state levels of Smad7/6 were higher in Tril morphants relative to controls (Fig. 5I). By contrast, steady-state levels of Smad6/7 were higher than those of wild-type Smad7 in control embryos, but were unchanged relative to wild-type Smad7 in Tril morphants. These results demonstrate that the N- and C-terminal halves of Smad7 are both required, and must be covalently linked for Tril-dependent degradation, and that the C-terminus, but not the N-terminus, of Smad6 can substitute for that of Smad7 in this process.

DISCUSSION

Gata2 and Bmps function together in multiple tissues and at multiple developmental stages to regulate hematopoiesis. In the current study, we identify Tril as a novel component of a Bmp-Gata2 positive-feedback loop that plays an essential role in enabling mesodermal precursors to commit to a hematopoietic fate.

During gastrulation, Bmps and Gata2 are required in both ectoderm and mesoderm for blood development. In the mesoderm, Bmps induce expression of the transcription factors *scl*, *cdx1* and *cdx4*, and these factors are necessary and sufficient to specify primitive erythroid fate (Lengerke et al., 2008; Mead et al., 1998). Bmps also induce expression of *gata2* in both germ layers (Friedle and Knochel, 2002; Maeno et al., 1996; Walmsley et al., 1994; Yan and Chen, 2011) and Gata2 is required downstream of Bmps to specify blood (Dalgin et al., 2007; Mimoto et al., 2015). Our current findings provide an explanation for why Gata2 is required downstream of Bmps in mesoderm, even though Bmps are sufficient to drive expression of the transcription factors that activate the hematopoietic program. Specifically, we have identified *tril* as a Gata2 target gene that triggers degradation of the Bmp inhibitor, Smad7. Thus, during normal development Bmps induce expression of *gata2*, which induces expression of *tril*. Tril then promotes degradation of endogenous Smad7 (Fig. 6C). Smad7 inhibits Bmp signaling at two levels: it interferes with Bmp receptor-mediated

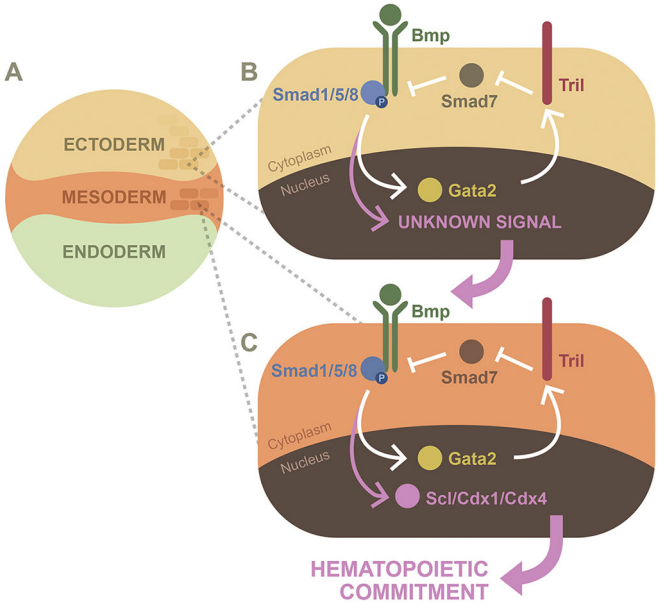

Fig. 6. Tril is a novel component of a Bmp-Gata2 positive-feedback loop. (A) Schematic illustration of germ layers in a gastrula stage embryo. (B,C) In ectodermal (B) and mesodermal (C) cells, Bmps induce expression of *gata2*, which induces expression of *tril*. Tril promotes degradation of Smad7, allowing for robust Bmp receptor-mediated activation of Smad1. In mesodermal cells, pSmad1/5/8 induces transcription of *Scl*, *cdx1* and *cdx4*, which initiate the hematopoietic program. In ectodermal cells, the transcriptional target of pSmad1/5/8 that signals to mesodermal cells (pink arrow) is unknown.

phosphorylation of Smad1/5/8, and also antagonizes pSmad1/5/8-dependent transcription in the nucleus (Yan and Chen, 2011). Thus, degradation of Smad7 not only allows for robust phosphorylation of Smad1/5/8, but also facilitates transcription of *scl*, *cdx1* and *cdx4*, which initiate the hematopoietic program. This explains how Tril can act both upstream and downstream of Smad1/5/8 phosphorylation to promote Bmp signaling. In the absence of Tril, Smad7 levels rise, dampening the transcriptional output of the Bmp pathway such that the hematopoietic program is not initiated in mesodermal cells.

The above model explains how the Gata2-Tril-Bmp feedback loop functions to drive hematopoietic specification in mesodermal cells, but our data show that the same feedback loop operates and is required in ectodermal cells in order for mesoderm to form blood (Fig. 6B). Although Bmp genes are highly expressed in ventral mesodermal cells that form most of the VBI, it is possible that ectodermal cells provide a secondary source of Bmp ligands that signal to the mesoderm, and that the Gata2-Tril-Bmp feedback loop is necessary to boost production of Bmps in ectodermal cells. Bmps have been shown to positively auto-regulate their own expression in various contexts (Hammerschmidt et al., 1996; Jones et al., 1992) and they may do so in ventral ectoderm. Alternatively, ectodermally derived Bmps may stimulate extracellular matrix (ECM) formation to augment Bmp delivery and/or signal reception within mesodermal cells. Various ECM components, including collagen, fibronectin and laminin have been shown to stimulate pathway activation in response to Bmp ligands (Endo et al., 2012; Paralkar et al., 1992) and Bmps can induce fibronectin expression and/or fibril assembly (Koli et al., 2004; Tang et al., 2003). Our data show that Tril is required for expression of *sizzled*, which controls fibronectin matrix deposition and thus Bmp responsiveness in the foregut of early *Xenopus* embryos (Kenny et al., 2012). It is also possible that Tril stimulates production of non-cell-autonomous

Development (2016) 143, 4016-4026 doi:10.1242/dev.141812

signals required for mesoderm to form blood, independent of its effects of Bmp signaling.

Our results show that Tril promotes downregulation of Smad7 protein. The ubiquitin ligase Smurf1 can stimulate degradation of Smad7 in some contexts, and our data showing that Smad7 lacking the Smurf binding motif displays enhanced accumulation in both wild-type and Tril morphant embryos suggest that Smurf1 promotes Smad7 degradation during development, but that this process does not require Tril. Instead, we show that Tril is required to keep Smad7 protein levels in check via a negative regulatory mechanism that requires both the N- and C-terminal domains of Smad7. Previous studies have shown that the C-terminal MH2 domain of Smad7 is the primary determinant of activity, and is sufficient for Bmp pathway inhibition, but that the N-terminal domain is essential for full activity and can physically interact with the isolated C-domain to enhance its activity (Hanyu et al., 2001; Nakayama et al., 2001). The C-terminal domain of Smad7 binds the ubiquitin ligase Arkadia, which can target Smad7 for proteasomal degradation (Koinuma et al., 2003). It is unlikely that Tril activates Arkadia to selectively degrade Smad7 since Arkadia also targets Smad6 (Tsubakihara et al., 2015), which is not affected in Tril morphants. Recently, the E3 ubiquitin ligase Rnf12 was shown to be a key negative regulator of Smad7 protein levels (Zhang et al., 2012). In *Xenopus*, *rnf12* is co-expressed with *tril* throughout the ectoderm and mesoderm during gastrulation (Hiratani et al., 2003). It is possible that Tril either activates Rnf12 or promotes nuclear export of Smad7, thereby making it accessible to Rnf12 and other cofactors that mediate degradation. Consistent with the latter possibility, Smad7 protein accumulates primarily in the nucleus of Tril morphants. Furthermore, our analysis of Smad7/6 chimeras demonstrates that the N-terminal domain of Smad7, which contains a region required for nuclear localization (Hanyu et al., 2001), is essential to confer susceptibility to Tril-mediated degradation.

Tril was originally identified as a co-receptor that interacts with Tlr3 and Tlr4 to activate the NF-κB transcription complex during innate immunity (Carpenter et al., 2009, 2011), but it is not known whether it functions in concert with Tlrs in all contexts. In *Drosophila*, Toll-mediated activation of NF-κB plays an essential role in dorsoventral patterning by inducing expression of Bmp antagonists and repressing expression of *decapentaplegic*, the fly ortholog of *bmp2/4* (Hong et al., 2008). There is some evidence that a homologous, maternally controlled Tlr pathway contributes to dorsal/ventral patterning in *Xenopus* (Prothmann et al., 2000) but Tril does not participate in this process since it functions zygotically to promote, rather than repress, Bmp signaling. To date, there is no evidence in any model system that Tlr-mediated activation of NF-κB is required to promote Bmp signaling during primitive hematopoiesis. Furthermore, we find no evidence that NF-κB activity is impaired in Tril morphants. However, Tlrs activate a diverse array of adaptor proteins, ubiquitin ligases and kinases in a context-dependent manner (Gay et al., 2014) and it is possible Tril functions in concert with Tlrs to activate a similar pathway that culminates in degradation of Smad7.

In contrast to the hematopoietic defects observed in *Xenopus* Tril morphants, mice lacking *tril* show impaired cytokine production in the brain in response to infection, but do not show gross developmental defects (Wochal et al., 2014). Tril may have subtle functions during mammalian development that have not yet been examined or other molecules present in mice, but not in *Xenopus*, may compensate for loss of Tril. Further studies will be required to determine whether Tril regulates Smad7 protein levels in mammals as it does in *Xenopus*.

MATERIALS AND METHODS

Xenopus embryo culture and manipulation

Animal procedures followed protocols approved by the University of Utah Institutional Animal Care and Use Committee. Embryos were obtained, microinjected and cultured as described (Moon and Christian, 1989). Embryo explants, tissue dissections and microarray analysis were performed as described (Mimoto et al., 2015). Embryos were stained for β-galactosidase activity using Red-gal (Research Organics) and processed for *in situ* hybridization as described (Harland, 1991), except that the vitelline coat was not removed prior to fixation and BM purple (Roche) was used as a substrate.

Morpholinos and cDNA constructs

A *Xenopus tril* cDNA was obtained using PCR-based approaches. NCBI accession numbers for *tril.S* and *tril.L* are KX377965 and KX377966, respectively. Gata2 (Dalgin et al., 2007), Smad7 (Choi et al., 2008), control and Tril MOs (Tril MO1: 5′-CCAAAATCTGGGCATCACCTTTC and Tril MO2: 5′-TCCCAAACTGCTTAAACTGTCAGCT) were purchased from Gene Tools (Philomath, OR). Mutant forms of Smad7-Myc have been described (Nakayama et al., 2001) except for Smad7K3A, which was generated using a QuikChange II XL site-directed mutagenesis kit (Agilent Technologies).

Immunoblots

Embryos were lysed in TNSG (20 mM Tris-HCl, pH 8.0, 137 mM NaCl, 10% glycerol, 1% NP-40; Hwang et al., 2013) or Triton X-100 lysis buffer (Choi and Han, 2005) containing HALT protease and phosphatase inhibitor cocktail (Thermo Fisher Scientific). Immunoblots were performed as described (Kwon and Christian, 2011) with the following antibodies: anti-phospho-Smad1/5 (Cell Signaling 9511S; 1:1000), anti-total Smad1/5 (Cell Signaling 9516; 1:1000), anti-Myc epitope [Developmental Studies Hybridoma Bank (DSHB), clone 9E10; 1:1000], anti-Flag epitope (Sigma clone M2, F1804; 1:1000), anti-phospho-ERK (Cell Signaling, 9106; 1:2000), anti-ERK (Cell Signaling 9102; 1:2000), and anti-β-Actin (Sigma A2066; 1:10,000).

Immunostaining

Ectodermal explants were fixed in 4% paraformaldehyde in PBS for 1 h at room temperature, washed three times in PBS for 15 min, incubated with anti-Myc antibody (DSHB, clone 9E10; 1:100) in PBT (1× PBS+0.1% Triton X-100) containing 10% sheep serum overnight at 4°C, followed by three 15 min washes in PBT. Explants were then incubated with Alexa Fluor 488-conjugated secondary antibody (Invitrogen, A11029; 1:1000) for 2 h at room temperature, washed three times in PBT for 15 min, and nuclei were stained with DAPI.

Analysis of RNA

Total RNA was isolated and northern analysis performed as described (Christian and Moon, 1993). qPCR (Mimoto et al., 2015) and semi-quantitative RT-PCR (Nakayama et al., 1998) was performed as described using an annealing temperature of 58°C. Primer sequences are listed in Table S1.

Statistical analysis

NIH ImageJ software was used to quantify band intensities. A Student's *t*-test was used to compare differences in gene expression or protein levels between two groups. Differences in subcellular localization of Smad7 were analyzed using GraphPad software to conduct two-way ANOVA followed by a Bonferroni multiple comparisons test. Differences with $P<0.05$ were considered statistically significant.

Acknowledgements

We thank Anne Martin for generating Fig. 6 and Chris Gregg, Kathryn Moore and Sungjin Park for helpful comments on the manuscript.

Competing interests

The authors declare no competing or financial interests.

Author contributions

Y.S.G. and J.L.C. designed and performed research, analyzed data and wrote the paper, S.K., M.S.M. and Y.X. performed research and analyzed data.

Data availability

cDNA sequences for *Xenopus tril.S* and *tril.L* are available in GenBank with accession numbers KX377965 and KX377966, respectively.

Funding

This work was supported by the National Institute of Child Health and Human Development [RO1HD067473 and RO3HD050242 to J.L.C., T32HD049309 to M.S.M.]; National Institute of Diabetes and Digestive and Kidney Diseases [T32DK007115 to Y.S.G.]; the Huntsman Cancer Foundation and the National Cancer Institute [P30CA042014]. This work utilized DNA, peptide and imaging shared resources supported by the Huntsman Cancer Foundation and the National Cancer Institute [P30CA042014]. The content is solely the responsibility of the authors and does not represent the official views of the National Institutes of Health. Deposited in PMC for release after 12 months.

Supplementary information

Supplementary information available online at
http://dev.biologists.org/lookup/doi/10.1242/dev.141812.supplemental

References

Bai, S. and Cao, X. (2002). A nuclear antagonistic mechanism of inhibitory Smads in transforming growth factor-beta signaling. *J. Biol. Chem.* **277**, 4176-4182.
Baron, M. H., Isern, J. and Fraser, S. T. (2012). The embryonic origins of erythropoiesis in mammals. *Blood* **119**, 4828-4837.
Belaoussoff, M., Farrington, S. M. and Baron, M. H. (1998). Hematopoietic induction and respecification of A-P identity by visceral endoderm signaling in the mouse embryo. *Development* **125**, 5009-5018.
Carpenter, S., Carlson, T., Dellacasagrande, J., Garcia, A., Gibbons, S., Hertzog, P., Lyons, A., Lin, L.-L., Lynch, M., Monie, T. et al. (2009). TRIL, a functional component of the TLR4 signaling complex, highly expressed in brain. *J. Immunol.* **183**, 3989-3995.
Carpenter, S., Wochal, P., Dunne, A. and O'Neill, L. A. J. (2011). Toll-like receptor 3 (TLR3) signaling requires TLR4 Interactor with leucine-rich REPeats (TRIL). *J. Biol. Chem.* **286**, 38795-38804.
Choi, S.-C. and Han, J.-K. (2005). Rap2 is required for Wnt/beta-catenin signaling pathway in Xenopus early development. *EMBO J.* **24**, 985-996.
Choi, S.-C., Kim, G.-H., Lee, S. J., Park, E., Yeo, C.-Y. and Han, J.-K. (2008). Regulation of activin/nodal signaling by Rap2-directed receptor trafficking. *Dev. Cell* **15**, 49-61.
Christian, J. L. and Moon, R. T. (1993). Interactions between Xwnt-8 and Spemann organizer signaling pathways generate dorsoventral pattern in the embryonic mesoderm of Xenopus. *Genes Dev.* **7**, 13-28.
Ciau-Uitz, A., Liu, F. and Patient, R. (2010). Genetic control of hematopoietic development in Xenopus and zebrafish. *Int. J. Dev. Biol.* **54**, 1139-1149.
Dale, L., Howes, G., Price, B. M. and Smith, J. C. (1992). Bone morphogenetic protein 4: a ventralizing factor in early Xenopus development. *Development* **115**, 573-585.
Dalgin, G., Goldman, D. C., Donley, N., Ahmed, R., Eide, C. A. and Christian, J. L. (2007). GATA-2 functions downstream of BMPs and CaM KIV in ectodermal cells during primitive hematopoiesis. *Dev. Biol.* **310**, 454-469.
Drevon, C. and Jaffredo, T. (2014). Cell interactions and cell signaling during hematopoietic development. *Exp. Cell Res.* **329**, 200-206.
Ebisawa, T., Fukuchi, M., Murakami, G., Chiba, T., Tanaka, K., Imamura, T. and Miyazono, K. (2001). Smurf1 interacts with transforming growth factor-beta type I receptor through Smad7 and induces receptor degradation. *J. Biol. Chem.* **276**, 12477-12480.
Endo, Y., Ishiwata-Endo, H. and Yamada, K. M. (2012). Extracellular matrix protein anosmin promotes neural crest formation and regulates FGF, BMP, and WNT activities. *Dev. Cell* **23**, 305-316.
Friedle, H. and Knochel, W. (2002). Cooperative interaction of Xvent-2 and GATA-2 in the activation of the ventral homeobox gene Xvent-1B. *J. Biol. Chem.* **277**, 23872-23881.
Gay, N. J., Symmons, M. F., Gangloff, M. and Bryant, C. E. (2014). Assembly and localization of Toll-like receptor signalling complexes. *Nat. Rev. Immunol.* **14**, 546-558.
Graff, J. M., Thies, R. S., Song, J. J., Celeste, A. J. and Melton, D. A. (1994). Studies with a Xenopus BMP receptor suggest that ventral mesoderm-inducing signals override dorsal signals in vivo. *Cell* **79**, 169-179.
Green, Y. S., Kwon, S. and Christian, J. L. (2016). Expression pattern of bcar3, a downstream target of Gata2, and its binding partner, bcar1, during Xenopus development. *Gene Expr. Patterns* **20**, 55-62.
Gronroos, E., Hellman, U., Heldin, C.-H. and Ericsson, J. (2002). Control of Smad7 stability by competition between acetylation and ubiquitination. *Mol. Cell* **10**, 483-493.
Hammerschmidt, M., Serbedzija, G. N. and McMahon, A. P. (1996). Genetic analysis of dorsoventral pattern formation in the zebrafish: requirement of a BMP-like ventralizing activity and its dorsal repressor. *Genes Dev.* **10**, 2452-2461.
Hanyu, A., Ishidou, Y., Ebisawa, T., Shimanuki, T., Imamura, T. and Miyazono, K. (2001). The N domain of Smad7 is essential for specific inhibition of transforming growth factor-beta signaling. *J. Cell Biol.* **155**, 1017-1028.
Harland, R. M. (1991). In situ hybridization: an improved whole-mount method for Xenopus embryos. *Methods Cell Biol.* **36**, 685-695.
Hiratani, I., Yamamoto, N., Mochizuki, T., Ohmori, S.-Y. and Taira, M. (2003). Selective degradation of excess Ldb1 by Rnf12/RLIM confers proper Ldb1 expression levels and Xlim-1/Ldb1 stoichiometry in Xenopus organizer functions. *Development* **130**, 4161-4175.
Hong, J.-W., Hendrix, D. A., Papatsenko, D. and Levine, M. S. (2008). How the Dorsal gradient works: insights from postgenome technologies. *Proc. Natl. Acad. Sci. USA* **105**, 20072-20076.
Hwang, Y.-S., Lee, H.-S., Kamata, T., Mood, K., Cho, H. J., Winterbottom, E., Ji, Y. J., Singh, A. and Daar, I. O. (2013). The Smurf ubiquitin ligases regulate tissue separation via antagonistic interactions with ephrinB1. *Genes Dev.* **27**, 491-503.
Jones, C. M., Lyons, K. M., Lapan, P. M., Wright, C. V. and Hogan, B. L. (1992). DVR-4 (bone morphogenetic protein-4) as a posterior-ventralizing factor in Xenopus mesoderm induction. *Development* **115**, 639-647.
Kavsak, P., Rasmussen, R. K., Causing, C. G., Bonni, S., Zhu, H., Thomsen, G. H. and Wrana, J. L. (2000). Smad7 binds to Smurf2 to form an E3 ubiquitin ligase that targets the TGF beta receptor for degradation. *Mol. Cell* **6**, 1365-1375.
Kenny, A. P., Rankin, S. A., Allbee, A. W., Prewitt, A. R., Zhang, Z., Tabangin, M. E., Shifley, E. T., Louza, M. P. and Zorn, A. M. (2012). Sizzled-tolloid interactions maintain foregut progenitors by regulating fibronectin-dependent BMP signaling. *Dev. Cell* **23**, 292-304.
Koinuma, D., Shinozaki, M., Komuro, A., Goto, K., Saitoh, M., Hanyu, A., Ebina, M., Nukiwa, T., Miyazawa, K., Imamura, T. et al. (2003). Arkadia amplifies TGF-beta superfamily signalling through degradation of Smad7. *EMBO J.* **22**, 6458-6470.
Koli, K., Wempe, F., Sterner-Kock, A., Kantola, A., Komor, M., Hofmann, W.-K., von Melchner, H. and Keski-Oja, J. (2004). Disruption of LTBP-4 function reduces TGF-beta activation and enhances BMP-4 signaling in the lung. *J. Cell Biol.* **167**, 123-133.
Kumano, G., Belluzzi, L. and Smith, W. C. (1999). Spatial and temporal properties of ventral blood island induction in Xenopus laevis. *Development* **126**, 5327-5337.
Kwon, S. and Christian, J. L. (2011). Sortilin associates with transforming growth factor-beta family proteins to enhance lysosome-mediated degradation. *J. Biol. Chem.* **286**, 21876-21885.
Lengerke, C., Schmitt, S., Bowman, T. V., Jang, I. H., Maouche-Chretien, L., McKinney-Freeman, S., Davidson, A. J., Hammerschmidt, M., Rentzsch, F., Green, J. B. A. et al. (2008). BMP and Wnt specify hematopoietic fate by activation of the Cdx-Hox pathway. *Cell Stem Cell* **2**, 72-82.
Lin, X., Liang, Y.-Y., Sun, B., Liang, M., Shi, Y., Brunicardi, F. C., Shi, Y. and Feng, X.-H. (2003). Smad6 recruits transcription corepressor CtBP to repress bone morphogenetic protein-induced transcription. *Mol. Cell. Biol.* **23**, 9081-9093.
Liu, F., Walmsley, M., Rodaway, A. and Patient, R. (2008). Fli1 acts at the top of the transcriptional network driving blood and endothelial development. *Curr. Biol.* **18**, 1234-1240.
Lyons, K. M., Jones, C. M. and Hogan, B. L. (1992). The TGF-beta-related DVR gene family in mammalian development. *Ciba Found. Symp.* **165**, 219-230; discussion 230-214.
Maeno, M. (2003). Regulatory signals and tissue interactions in the early hematopoietic cell differentiation in Xenopus laevis embryo. *Zool. Sci.* **20**, 939-946.
Maeno, M., Ong, R. C., Xue, Y., Nishimatsu, S.-I., Ueno, N. and Kung, H.-F. (1994). Regulation of primary erythropoiesis in the ventral mesoderm of Xenopus gastrula embryo: evidence for the expression of a stimulatory factor(s) in animal pole tissue. *Dev. Biol.* **161**, 522-529.
Maeno, M., Mead, P. E., Kelley, C., Xu, R. H., Kung, H. F., Suzuki, A., Ueno, N. and Zon, L. I. (1996). The role of BMP-4 and GATA-2 in the induction and differentiation of hematopoietic mesoderm in Xenopus laevis. *Blood* **88**, 1965-1972.
Mead, P. E., Kelley, C. M., Hahn, P. S., Piedad, O. and Zon, L. I. (1998). SCL specifies hematopoietic mesoderm in Xenopus embryos. *Development* **125**, 2611-2620.
Mimoto, M. S., Kwon, S., Green, Y. S., Goldman, D. and Christian, J. L. (2015). GATA2 regulates Wnt signaling to promote primitive red blood cell fate. *Dev. Biol.* **407**, 1-11.
Moon, R. T. and Christian, J. L. (1989). Microinjection and expression of synthetic mRNAs in *Xenopus* embryos. *Technique* **1**, 76-89.
Murakami, G., Watabe, T., Takaoka, K., Miyazono, K. and Imamura, T. (2003). Cooperative inhibition of bone morphogenetic protein signaling by Smurf1 and inhibitory Smads. *Mol. Biol. Cell* **14**, 2809-2817.
Myers, C. T. and Krieg, P. A. (2013). BMP-mediated specification of the erythroid lineage suppresses endothelial development in blood island precursors. *Blood* **122**, 3929-3939.

Development (2016) 143, 4016-4026 doi:10.1242/dev.141812

Nakayama, T., Snyder, M. A., Grewal, S. S., Tsuneizumi, K., Tabata, T. and Christian, J. L. (1998). Xenopus Smad8 acts downstream of BMP-4 to modulate its activity during vertebrate embryonic patterning. *Development* **125**, 857-867.

Nakayama, T., Berg, L. K. and Christian, J. L. (2001). Dissection of inhibitory Smad proteins: both N- and C-terminal domains are necessary for full activities of Xenopus Smad6 and Smad7. *Mech. Dev.* **100**, 251-262.

Paralkar, V. M., Weeks, B. S., Yu, Y. M., Kleinman, H. K. and Reddi, A. H. (1992). Recombinant human bone morphogenetic protein 2B stimulates PC12 cell differentiation: potentiation and binding to type IV collagen. *J. Cell Biol.* **119**, 1721-1728.

Prothmann, C., Armstrong, N. J. and Rupp, R. A. W. (2000). The Toll/IL-1 receptor binding protein MyD88 is required for Xenopus axis formation. *Mech. Dev.* **97**, 85-92.

Souchelnytskyi, S., Nakayama, T., Nakao, A., Moren, A., Heldin, C.-H., Christian, J. L. and ten Dijke, P. (1998). Physical and functional interaction of murine and Xenopus Smad7 with bone morphogenetic protein receptors and transforming growth factor-beta receptors. *J. Biol. Chem.* **273**, 25364-25370.

Tang, C.-H., Yang, R.-S., Liou, H.-C. and Fu, W.-M. (2003). Enhancement of fibronectin synthesis and fibrillogenesis by BMP-4 in cultured rat osteoblast. *J. Bone Miner. Res.* **18**, 502-511.

Tran, H. T., Sekkali, B., Van Imschoot, G., Janssens, S. and Vleminckx, K. (2010). Wnt/beta-catenin signaling is involved in the induction and maintenance of primitive hematopoiesis in the vertebrate embryo. *Proc. Natl. Acad. Sci. USA* **107**, 16160-16165.

Tsubakihara, Y., Hikita, A., Yamamoto, S., Matsushita, S., Matsushita, N., Oshima, Y., Miyazawa, K. and Imamura, T. (2015). Arkadia enhances BMP signalling through ubiquitylation and degradation of Smad6. *J. Biochem.* **158**, 61-71.

Tsukamoto, S., Mizuta, T., Fujimoto, M., Ohte, S., Osawa, K., Miyamoto, A., Yoneyama, K., Murata, E., Machiya, A., Jimi, E. et al. (2014). Smad9 is a new type of transcriptional regulator in bone morphogenetic protein signaling. *Sci. Rep.* **4**, 7596.

Walmsley, M. E., Guille, M. J., Bertwistle, D., Smith, J. C., Pizzey, J. A. and Patient, R. K. (1994). Negative control of Xenopus GATA-2 by activin and noggin with eventual expression in precursors of the ventral blood islands. *Development* **120**, 2519-2529.

Walters, M. J., Wayman, G. A. and Christian, J. L. (2001). Bone morphogenetic protein function is required for terminal differentiation of the heart but not for early expression of cardiac marker genes. *Mech. Dev.* **100**, 263-273.

Wilt, F. H. (1965). Erythropoiesis in the chick embryo: the role of endoderm. *Science* **147**, 1588-1590.

Wochal, P., Rathinam, V. A. K., Dunne, A., Carlson, T., Kuang, W., Seidl, K. J., Hall, J. P., Lin, L.-L., Collins, M., Schattgen, S. A. et al. (2014). TRIL is involved in cytokine production in the brain following Escherichia coli infection. *J. Immunol.* **193**, 1911-1919.

Yan, X. and Chen, Y.-G. (2011). Smad7: not only a regulator, but also a cross-talk mediator of TGF-beta signalling. *Biochem. J.* **434**, 1-10.

Zhang, L., Huang, H., Zhou, F., Schimmel, J., Pardo, C. G., Zhang, T., Barakat, T. S., Sheppard, K.-A., Mickanin, C., Porter, J. A. et al. (2012). RNF12 controls embryonic stem cell fate and morphogenesis in zebrafish embryos by targeting Smad7 for degradation. *Mol. Cell* **46**, 650-661.

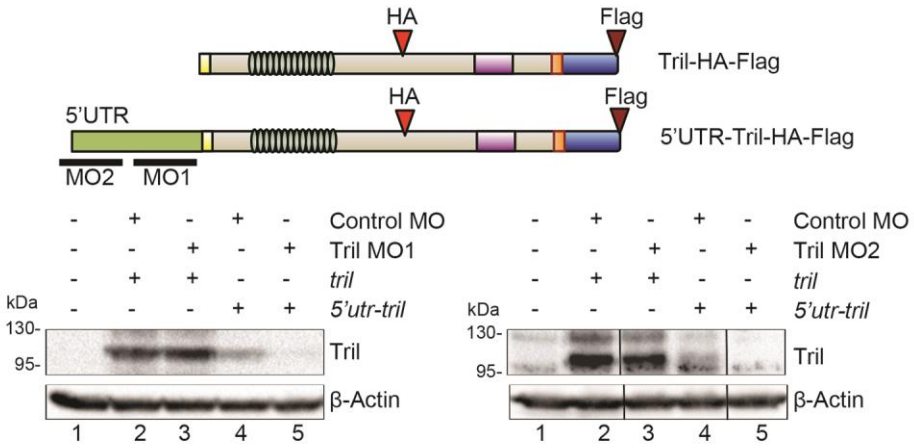

Figure S1. Two independent antisense MOs block translation of *tril* in vivo. Schematic illustration of epitope tagged Tril constructs. Regions where Tril MOs bind are indicated by the black bars. RNA encoding HA- and FLAG-epitope tagged Tril that lacks (Tril) or includes (5'UTR-Tril) the 5'UTR was coinjected into two-cell embryos together with control or Tril MOs. Immunoblots of lysates from injected embryos were probed with anti-HA (left panel) or anti-FLAG (right panel) antibodies and then reprobed for Actin as a loading control. Steady state levels of Tril protein generated from RNAs lacking the 5'UTR were reproducibly higher than those generated by RNAs that include the 5'UTR, suggesting that elements in the 5' UTR negatively regulate translation. Intervening lanes were removed using Photoshop (between lanes 2 and 3, and between lanes 4 and 5; marked by black bars) on the blot shown on the right.

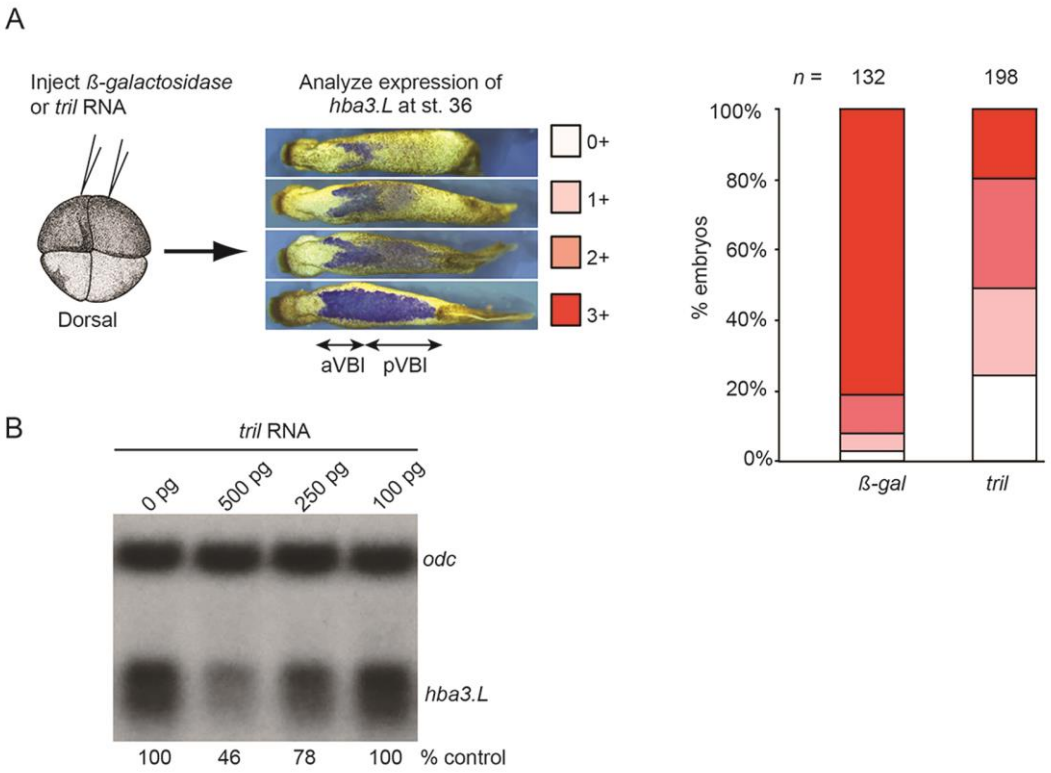

Figure S2. Upregulation of Tril leads to a reduction in blood. (A) RNA encoding ß-galactosidase (ß-gal) as a RNA injection control or Tril (1 ng) was injected into both ventral cells of 4-cell embryos as illustrated and expression of *globin* was analyzed by WMISH at stage 34. *Globin* staining in the posterior VBI (pVBI) of experimental embryos was scored as not detectable (0+), barely detectable (1+), moderately decreased (2+) or strong (3+) using the scale illustrated above the graph. aVBI; anterior VBI. (B) Tril RNA was injected into two ventral blastomeres of four-cell embryos and expression of *globin* was analyzed by Northern blotting at stage 34. Levels of *globin* transcripts are normalized to *odc* and reported as a percentage of *globin* levels in uninjected control embryos below each lane.

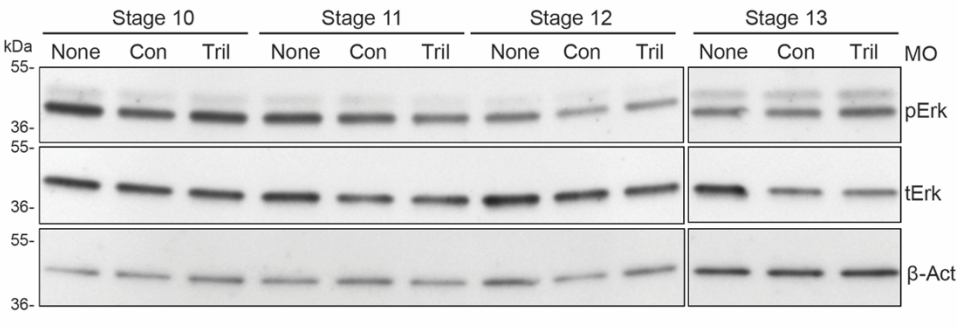

Figure S3. Tril is not required for activation of Erk. Control (CON), Tril, or no MO (NONE) was injected into both cells of two-cell embryos. Levels of phosphoErk (pErk), total Erk (tErk) and ß-Actin were analyzed by immunoblot of embryonic lysates at stage 10, 11, 12 and 13.

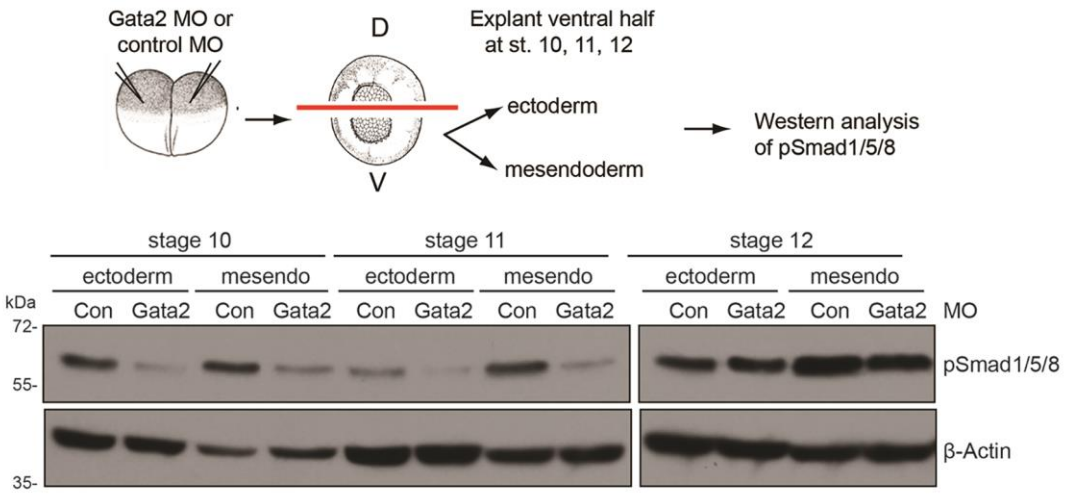

Figure S4. Gata2 is required for phosphorylation of Smad1 in ventral ectodermal and mesodermal cells during gastrulation. (A) Control (Con) or Gata2 MOs (40 ng) were injected into both cells of two-cell embryos. The ventral half was isolated from ten embryos in each group, and dissected into ectoderm or mesendoderm at stage 10, 11 and 12, as illustrated. Levels of pSmad1and ß-Actin (a loading control) were analyzed by immunoblot. Results were reproduced in two additional experiments.

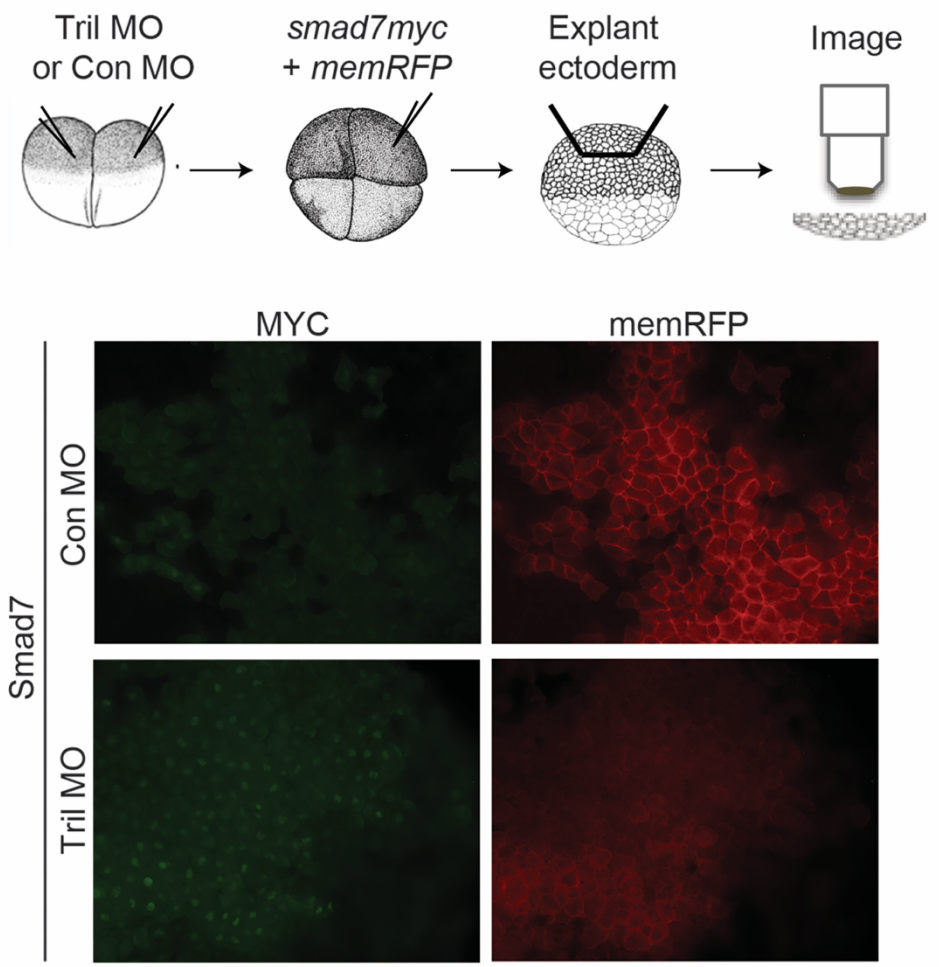

Figure S5. Smad7 signal is stronger in Tril morphants. Tril or control MOs (40 ng) were injected into both cells of two cell embryos and RNA encoding Smad7myc together with RNA encoding membrane targeted RFP (memRFP) was injected near the animal pole of a single blastomere at the four-cell stage. Ectoderm was explanted at st. 11 and immunostained for myc and RFP. Representative immunostaining photographed under identical conditions is shown.

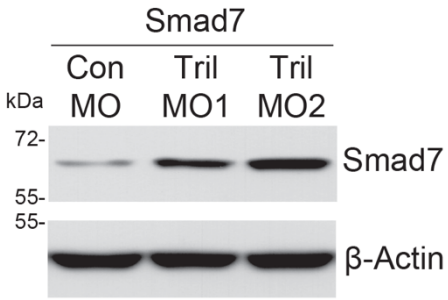

Figure S6. Smad7 levels are upregulated in embryos injected with two independent Tril MOs. RNA (50 pg) encoding Smad7myc was injected into two-cell embryos along with control or Tril MOs. Immunoblots of lysates from st. 11 embryos were probed with anti-myc antibodies, and then reprobed for Actin as a loading control.

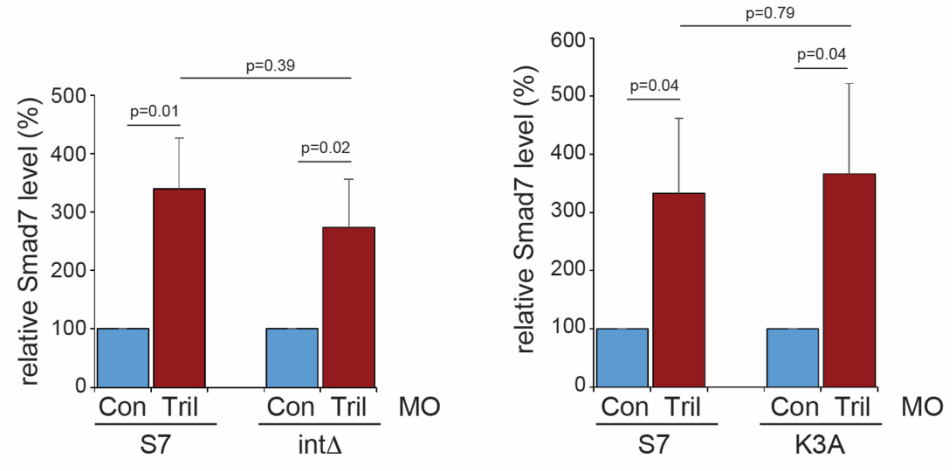

Fig. S7. Tril function of Smad7 degradation does not depend on Smurf1/2. RNA encoding Smad7myc (25 pg), Smad7intΔmyc (22 pg), or Smad7K3A (25 pg) was injected into two-cell embryos along with control or Tril MOs. Immunoblots of lysates from ten pooled st. 11 embryos in each group were probed with anti-myc antibodies, and then reprobed for ß-Actin. Levels of wild type or mutant Smad7 in Tril morphants (normalized to ß-Actin) are graphed as a percentage of levels in control morphants (three experiments, mean ± s.d., data analyzed by two tailed *t*-test).

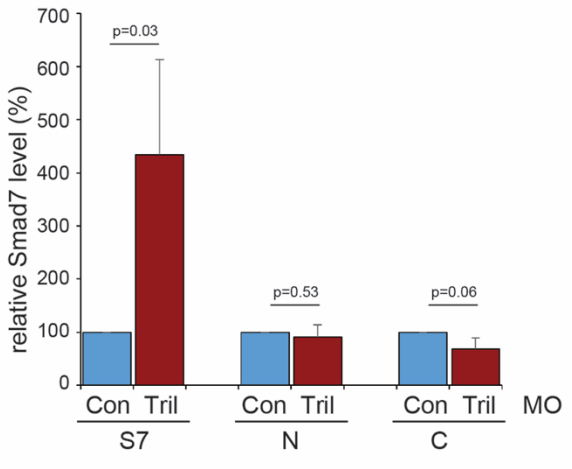

Fig. S8. Tril triggers degradation of Smad7 protein through a mechanism that requires both the amino- and carboxy-terminal regions of Smad7. RNA encoding Smad7myc (25 pg), Smad7Nmyc (1.4 pg) or Smad7Cmyc (0.5 pg) was injected into two-cell embryos along with control or Tril MOs. Immunoblots of lysates from st. 11 embryos were probed with anti-myc antibodies, and then reprobed for Actin. Levels of wild type or mutant Smad7 in Tril morphants (normalized to ß-Actin) are graphed as a percentage of levels in control morphants (three experiments, mean ± s.d., data analyzed by two tailed *t*-test).

Table S1. Primers used for PCR. Related to Experimental Procedures

Primer Name	Sequence
tril F	ACC AAG TGC TGG CTT TAT CG
tril R	GGG GAC GAT GAG ACT GAA AA
scl F	TGC TCT ATG GGC TCA ATC AG
scl R	GGG ACC TTC AGA GAT TTC CA
msx1 F	AGC TTG GCA CAA CCA CAG AA
msx1 R	CGA AAT GCA AAC AGA CAG TGC T
ventx2 F	GGA AAC TCG CAG CCA AAC TC
ventx2 R	ACC TGG GTA GGG ATG TTG GA
t (xbra) F	TTC TGA AGG TGA GCA TGT CG
t (xbra) R	GTT TGA CTT TGC TAA AAG AGA CAG G
szl F (for RT-PCR)	CTG ACA CTT GCC ACA AGG AGG
szl R (for RT-PCR)	GCA TGG TAA TGG GAT GCG CTC
szl F (for qPCR)	CCG AAG GCC CAG TTG AGT TC
szl R (for qPCR)	TCT GCC AGT GGA AAA CCC TG
hba3.L (globin) F	GTG ACC TGC ATG CCT ACA AC
hba3.L (globin) R	ACC TCA GCC AGG AAT TTG TC
smad7 F	TGG GAG ACC TGA TTG GTT GC
smad7 R	GTA GGG GTT GTG GGT CTT GG
odc F	TGC AGA GCC TGG GAG ATA CT
odc R	CAT TGG CAG CAT CTT CTT CA